

Minireview

Functional imaging: what evidence is there for its utility in clinical trials of targeted therapies?

N Tunariu^{*,1}, SB Kaye² and NM deSouza¹

¹Section of Clinical Magnetic Resonance, The Institute of Cancer Research and Royal Marsden NHS Foundation Trust, Sutton, Surrey SM2 5PT, UK;
²Drug Development Unit, The Institute of Cancer Research and Royal Marsden NHS Foundation Trust, Sutton, Surrey SM2 5PT, UK

Key issues in early clinical trials of targeted agents include the determination of target inhibition, rational patient selection based on pre-treatment tumour characteristics, and assessment of tumour response in the absence of actual shrinkage. There is accumulating evidence that functional imaging using advanced techniques such as dynamic contrast enhanced (DCE)-magnetic resonance imaging (MRI), DCE-computerised tomography (CT) and DCE-ultrasound, diffusion weighted-MRI, magnetic resonance spectroscopy and positron emission tomography-CT using various labelled radioactive tracers has the potential to address all three. This article reviews this evidence with examples from trials using targeted agents with established clinical efficacy and summarises the clinical utility of the various techniques. We therefore recommend that input from specialist radiologists is sought at the early stages of trial design, in order to ensure that functional imaging is incorporated appropriately for the agent under study. There is an urgent need to strengthen the evidence base for these techniques as they evolve, and to ensure standardisation of the methodology.

British Journal of Cancer (2012) **106**, 619–628. doi:10.1038/bjc.2011.579 www.bjcancer.com

Published online 26 January 2012

© 2012 Cancer Research UK

Keywords: phase I trial; imaging biomarker; targeted agents; multiparametric imaging

An increasing knowledge about the major pathways dysregulated in cancer has resulted in a large array of targeted pathway inhibitors submitted for phase I trials. Recent figures suggest that <10% of new molecules reach the market primarily because of a lack of demonstrable clinical activity (Kola and Landis, 2004). Other contributing factors include lack of appropriate quantitative imaging methods to guide both preclinical and clinical development. The standard imaging assessment of tumour response relies on size measurements, which, with predominantly cytostatic targeted agents, may not reflect the drug effect. The wide therapeutic index of targeted agents, non-linear relationship between dose and effect and non-mechanism related toxicity may require definition of an optimal biological dose rather than a maximal tolerated dose (MTD). Also, many of these agents may prove to be more effective in combination therapy either with synergistic targeted agents or with chemotherapy and the minimum biologically active dose needs also to be determined. Moreover, because targeted agents are approved for cancer treatment largely based on marginal benefits shown in clinical trials, it means that a large percentage of patients may merely suffer toxicity without therapeutic benefit.

Functional imaging biomarkers have the potential to quantify biological characteristics of tumours and measure on-target and off-target effects that indicate early likelihood of response to a specific therapy, which can then be used to guide the optimal biological dose and drug schedule. Serial, non-invasive assessments of whole tumour are possible. This is particularly important in the context of inter and intra-patient tumour heterogeneity as

different parts of the tumour and primary vs metastatic lesions may be biologically different and these characteristics may change with treatment. This article reviews currently available functional imaging methods and discusses their potential for stratifying patients for targeted therapies and assessment of tumour response by measuring on-target and off-target effects. PubMed searches for the terms phase I trial, RECIST, antiangiogenic, cytostatic, molecular imaging, dynamic contrast enhanced (DCE)-magnetic resonance imaging (MRI), diffusion weighted (DW)-MRI, DCE-ultrasound (US), FDG-positron emission tomography (PET), treatment response and derivative references, were performed. Abstracts and articles judged most relevant to the goals of this report were reviewed with emphasis on limitations and strengths of the imaging approaches to treatment response assessment.

FUNCTIONAL IMAGING MEASUREMENTS AND TERMINOLOGY

The biological features of a tumour, for example, vascularity, hypoxia, cell turnover determine its characteristics on functional imaging. The currently available imaging techniques available in the clinic for identifying tumour characteristics are MRI, PET, computerised tomography (CT) and US. Most of the functional techniques use an additional external contrast agent or radioactive tracer. Figure 1 summarises the commonly used imaging techniques and shows the quantitative readouts obtained.

Imaging angiogenesis (blood flow and vascular permeability)

Perfusion imaging techniques exploit pathophysiological differences between 'leaky', disorganised, tumour neovessels and

*Correspondence: Dr N Tunariu; E-mail: nina.tunariu@icr.ac.uk

Received 2 September 2011; revised 25 November 2011; accepted 7 December 2011; published online 26 January 2012

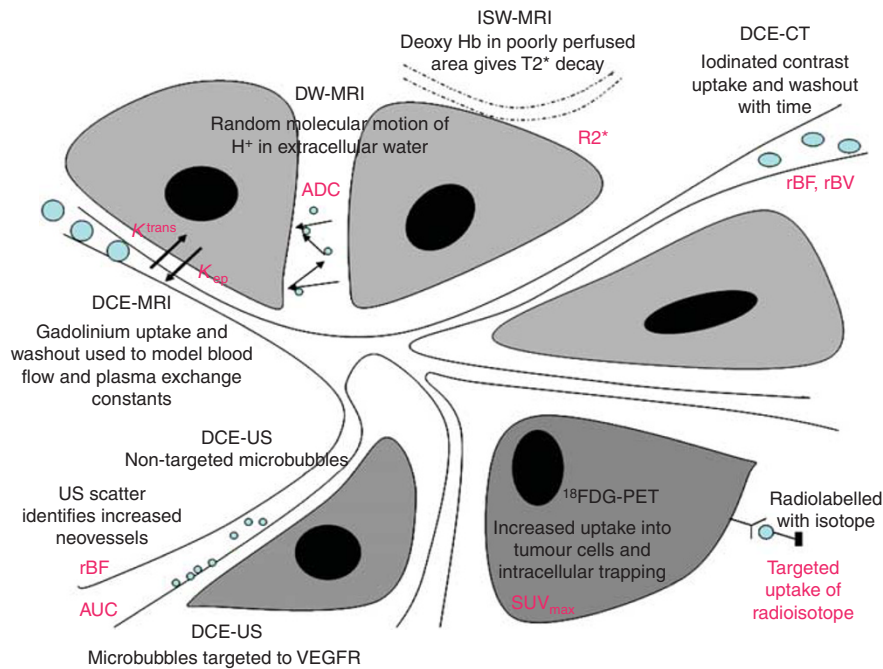


Figure 1 Schematic showing the currently most used functional techniques in the clinic and illustrating their mechanism of action. The output measures from each of these are shown in pink. Dynamic contrast enhanced MRI with output measured as rate constants (K^{trans} and K_{ep}) of gadolinium transfer between intravascular and extravascular compartments measured in ml min^{-1} . Diffusion weighted MRI with measured apparent diffusion coefficient (ADC) measured in $\text{mm}^2 \text{s}^{-1}$. Intrinsic susceptibility weighted MRI with output the relaxation rate constant $R2^*$ measured in s^{-1} . Dynamic contrast enhanced CT, with output of relative blood flow (rBF) and relative blood volume (rBV) measured in ml min^{-1} and ml , respectively. Parameters in PET are measured as maximum standardised uptake values (SUV_{max}) of the radioligand. In US, quantified parameters are change in US backscatter before and after injection of microbubbles and represented as integrated area under the curve (AUC) and rBF.

normal, well-organised vasculature. Serial images are acquired dynamically, through a volume of interest before, during and after administration of a contrast agent: gadolinium for MRI, iodinated contrast for CT and microbubbles for US. The acquired data are fitted to mathematical models to obtain quantitative parameters. The techniques are relatively simple to perform on standard clinical systems (1.5 Tesla for MRI, standard multidetector CT and most of the modern US machines) but require strict protocols, careful acquisition, accurate contrast agent dosing and injection rate, image timing, and image analysis for quantification.

The most common methods of perfusion imaging are dynamic contrast-enhanced (DCE) and dynamic susceptibility contrast (DSC) MRI, the latter being used almost exclusively in brain imaging. Magnetic resonance imaging sequences are designed to be sensitive to the presence of contrast medium in the extravascular space (EES) on DCE-MRI (T1 or relaxivity-based methods) or to the vascular phase of contrast medium delivery (T2 or susceptibility-based methods) on DSC-MRI. For DCE-MRI, the resulting signal intensity within the tumour reflects a composite of overall perfusion, vessel permeability or 'leakiness' and the volume of EES. A recent consensus meeting has recommended the following readouts: volume transfer constant of contrast between the blood plasma and the EES (K^{trans}), size of the EES (v_e) and IAUGC (area under the Gadolinium curve) for assessing anti-angiogenic and vascular disrupting agents in clinical trials (Leach *et al*, 2005). K^{trans} is often used as a marker for the permeability of tumour vasculature. Related measures such as the rate constant (k_{ep}), which describes the ratio of K^{trans}/v_e , have also been used. For DSC-MRI, the degree of signal loss observed is dependent on the vascular concentration of the contrast agent and tumour perfusion; the most common used parameters are relative cerebral blood volume (BV), relative cerebral blood flow (BF) (Pope *et al*, 2011).

The data from DCE-CT imaging has a high spatial resolution and is potentially more quantitative than MRI as the change in CT

image intensity is linearly related to the concentration of the contrast agent. The technique also benefits from FDA-approved software platforms embedded in standard CT reporting workstations. However, there is always a trade-off between the radiation dose and image quality and the contrast dose (potentially nephrotoxic) is relatively high, resulting in a limited use of CT for repeated scanning. The commonly used parameters include: BF, BV, MTT (mean transit time) and permeability (Goh *et al*, 2006).

Dynamic contrast enhanced-US has been used to measure haemodynamics in human tumours over the last decade. The contrast agent consists of phospholipid-based microbubbles with a mean diameter on the order of $0.5-10 \mu\text{m}$ that encapsulate an inert gas, which when exposed to an US pulse, generate nonlinear resonances that allow enhanced representation of the vasculature. Microbubbles remain strictly intravascular following administration and therefore generated echoes relate to the flow within functional vessels. Most commonly, a 3-min acquisition is performed through a limited area within the tumour. The time-intensity curve in the region of interest depends on perfusion and is fitted to a kinetic model to determine volume and flow rate and semi-quantitative parameters such as peak intensity, time to peak intensity, MTT, area under the total enhancement curve (Lamuraglia *et al*, 2010), with most scanners offering data analysis software. However, DCE-US is still in its infancy and greatly operator dependent.

Amongst, positron-emitting tracers, H_2^{15}O -PET can be used to study tumour BF. Being a freely diffusible tracer, H_2^{15}O concentration shows a linear relation with signal intensity as measured with PET and the technique is thought to be able to absolutely quantify tumour perfusion (de Langen *et al*, 2008). A dynamic H_2^{15}O -PET scan acquisition takes 10 min and starts simultaneously with the bolus injection. The tracer has a short radioactive half-life of approximately 2 min, which allows repeated imaging after a short time or in combination with other tracers but requires an on-site cyclotron. The radiation dose is similar to that of ^{18}F -fluorodeoxyglucose (^{18}F -FDG)-PET.

Imaging hypoxia

Hypoxia is a clinically important cancer hallmark, being associated with increased resistance to treatment and poor survival. ^{18}F -labelled fluoromisonidazole (^{18}F -FMISO) is the most extensively studied PET tracer for imaging tissue oxygenation. Its use in clinical practice has been hindered by its relatively poor signal to noise ratio because of slow specific accumulation as well as slow clearance from normoxic tissues (Mees *et al*, 2009). Next-generation PET tracers like ^{18}F -labelled fluoroazomycin arabinoside have been developed and used successfully in head and neck cancer (Souvatzoglou *et al*, 2007).

Intrinsic susceptibility weighted (ISW)-MRI also known as BOLD (blood oxygenation level dependent)-MRI relies on the paramagnetic properties of deoxyhaemoglobin, to generate contrast because of the increased MR transverse relaxation rate ($R2^*$). The technique is sensitive to $p\text{O}_2$ within and in tissues adjacent to perfused vessels and can be easily quantified but does not measure $p\text{O}_2$ directly. pH, carbon dioxide tension and haematocrit can affect $R2^*$ readings and for correct interpretation of ISW-MRI the BV in the tissues of interest must be known (Padhani *et al*, 2007). More recently, it has been shown by analysing rapidly acquired DCE-MRI data with a specific kinetic model, it is also possible to obtain specific readouts of perfusion and permeability, which correlate with VEGF tumour expression and hypoxia (Donaldson *et al*, 2011).

Imaging tumour cell proliferation, death and necrosis

Diffusion weighted-MRI exploits intrinsic contrast arising from the thermal displacement of water molecules over a given time. In biologic tissues, the movement of water molecules is hindered because their motion is limited by interactions with cell membranes and macromolecules. The quantified apparent diffusion coefficient (ADC), has been correlated with cellular density, presence of necrosis and in the therapy setting, tumour cell apoptosis and proliferation indices (Padhani *et al*, 2009). A low ADC reflects impeded diffusion and can be found in highly cellular tissues or fibrosis. If there are areas of significant necrosis this results in less restriction of motion and therefore a high ADC.

3'-Deoxy-3'-[^{18}F]fluorothymidine (^{18}F -FLT) PET had initial encouraging results as a potential biomarker for tumour proliferation. Currently, there is not enough data to support its use for reliable assessment of therapy response (Barwick *et al*, 2009).

Imaging tumour metabolism

^{18}F -fluorodeoxyglucose, a glucose analogue that allows mapping of tumour glucose use is widely used both in routine clinical practice and clinical trials. A decrease in the maximum standard glucose uptake value – SUV max, most commonly used quantitative parameter, has been associated with treatment response to numerous anticancer therapies (Shankar *et al*, 2006). More recently, it has been shown that Akt activation causes disruption to transcription of the glucose transporter GLUT1 and its translocation to the plasma membrane and promotes glucose utilisation independent of the effects on cell proliferation (Ma *et al*, 2009). ^{18}F -FDG-PET has therefore been proposed as a pharmacodynamic biomarker for assessing efficacy of on-target inhibition of the PI3K/Akt pathway.

Pre and clinical hydrogen magnetic resonance spectroscopy (^1H -MRS) studies have demonstrated that proliferating cells and many tumours display elevated choline signals. The method has been successfully used in characterisation and detection of brain and prostate cancer and there is some evidence towards its use as a response biomarker following chemotherapy in breast cancer (Baek *et al*, 2009). There is yet not enough evidence to support the role of MRS as a potential biomarker in phase I trials, although

preclinical data are emerging (Belouche-Babari *et al*, 2010), highlighting its potential.

EVIDENCE FOR USE OF FUNCTIONAL IMAGING IN PATHWAY-SPECIFIC TARGETED AGENTS

Measuring on-target effects on vasculature

Non-targeted microbubbles DCE-US after administration of a single dose (41 mg kg^{-1}) of a combrestatin A4 derivative, AVE8062 in melanoma-bearing nude mice (which causes a rapid and selective shutdown of tumour neovasculature resulting in ischaemia and extensive haemorrhagic necrosis in xenografts) showed that intratumoural vessel depletion started 15-min post injection and was maximal at 6 h. This enabled planning of a clinical phase I assessment with DCE-US at 6- and 24-h post drug (Lavisse *et al*, 2008). Similar results were shown on clinical DCE-MRI, with the administration of CA4P causing a rapid reduction in K^{trans} and IAUGC at 4–6 h, which recovered by 24 h (Galbraith *et al*, 2003). A significant reduction in tumour BF and BV 30 min after treatment with CA4P (Anderson *et al*, 2003) has also been seen on H_2^{15}O -PET and ^{15}O -CO PET. Notably, the effect on BV was still present at 24 h while the effect on BF was observed only in patients receiving larger doses of CA4P.

The downstream effects of VEGFR inhibition on DCE-MRI have been documented in >40 phase I trials (Figure 2) with a significant reduction in K^{trans} and/or IAUGC being reported with multiple agents (Zweifel and Padhani, 2010). An interesting observation is that while the combination of VEGF and PDGF inhibitors has been associated with increased tumour vessel regression (Erber *et al*, 2004), the extent of associated change in DCE-MRI parameters with this combination of agents is variable or nonsignificant. This has been ascribed to the pro-permeability effects of PDGF inhibition by blocking pericytes recruitment to vessel walls and therefore reducing the vascular normalisation, and the associated reduction in K^{trans} (Erber *et al*, 2004).

A first phase I clinical trial using a humanised version of a mouse monoclonal anti-VEGF antibody HuMV833 labelled with ^{124}I showed a marked heterogeneity in receptor expression both between and within patients with a three-fold variation in

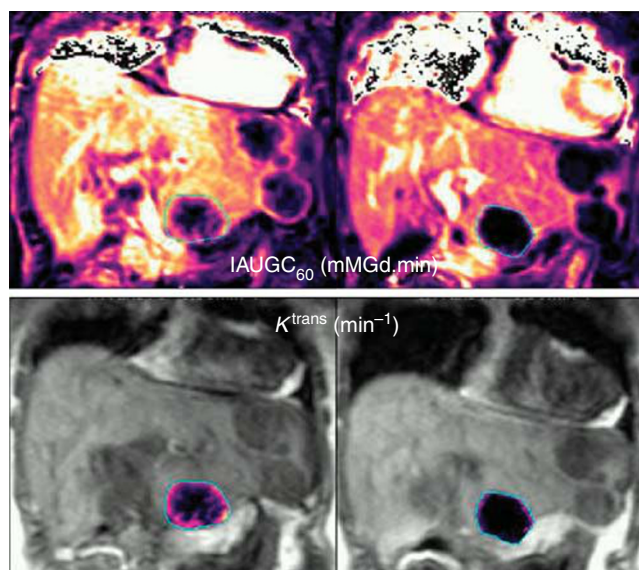


Figure 2 Dynamic contrast enhanced-MRI parametric maps before (left column) and 28 days after (right column) VEGF inhibitor therapy in a patient with metastatic colorectal carcinoma illustrating a down-stream effect with significant reduction in tumour vascularity (Courtesy to Dr C Messiou & M Orton, Royal Marsden Hospital).

HuMV833 concentration within individual tumours indicating that response to these agents is likely to mirror this heterogeneity and therefore impact significantly on dose-response assessments (Jayson *et al*, 2002). Integrin labelled PET tracers and labelled microbubbles and paramagnetic nanoparticles coated with small peptidic $\alpha_v\beta_3$ antagonists as MRI contrast agents have been described (Cai *et al*, 2005) but are still in experimental phase.

Correlations between reduction in vascularity on functional imaging such as DCE-MRI and DCE-US following antiangiogenic treatment and patient benefit have been reported in a small number of studies and warrant further exploration (Flaherty *et al*, 2008; Lassau *et al*, 2010; Jiang *et al*, 2012).

Measuring off-target effects on vasculature

The early reduction of K^{trans} on DCE-MRI in orthotopic mammary xenografts following treatment with a dual PI3K/mTOR inhibitor supports the biological observation that dysregulated angiogenesis and high tumour vascular permeability are in part PI3K dependent (Schnell *et al*, 2008). Although a decrease in the tumour perfusion by growth inhibition was reported on DCE-US following treatment with the mTOR inhibitor everolimus (5 mg kg⁻¹ for 3 weeks) (Broillet *et al*, 2005), other data show that K^{trans} did not change in everolimus-treated tumour models when compared with measurable changes seen with the VEGF inhibitor vatalanib (Lane *et al*, 2009). However, the impact of mTOR inhibition with rapamycin analogues on the PI3K/Akt pathway is complex, and may actually involve increased Akt pathway activation (O'Reilly, 2006).

Inhibition of HIF-1 α has dramatic effects on tumour vasculature: a dramatic reduction in tumour blood vessel permeability was seen on DCE-MRI in tumour-bearing mice within 2 h of treatment with PX-478 (Jordan *et al*, 2005).

Measuring on-target effects on metabolism

On-target effects of EGFR inhibition have been explored with radionuclide labelled agents in PET, for example, ¹²⁴I, ¹¹C or ¹⁸F-gefitinib. ¹⁸F-FDG-PET response has been correlated with Akt inactivation and plasma membrane GLUT1 expression in a study with mTOR inhibitors (Ma *et al*, 2009).

Measuring off-target effects on metabolism

The effect of antiangiogenic agents on ¹⁸F-FDG uptake has been explored with reduction in SUV_{max} being reported amongst others with sorafenib (Siemerink *et al*, 2008) and CA4P (Anderson *et al*, 2003).

In the clinic, downstream effects of EGFR inhibitors have been imaged with ¹⁸F-FDG-PET. Early changes in the SUV_{max} at 2 days after gefitinib treatment associated with progression-free survival (PFS) of 12 months were seen in a small study (Sunaga *et al*, 2008). ¹⁸F-FLT has also been found to predict response and patient outcome (positive and negative predictive values 92.9%) to EGFR inhibitors with a reduction in SUV_{max} of >10.4% at 7 days post gefitinib therapy predicting RECIST response on CT at 6 weeks (Sohn *et al*, 2008).

STRATIFYING PATIENTS FOR TARGETED THERAPIES USING FUNCTIONAL IMAGING

Functional imaging provides additional information on tumour characterisation, which could help in the selection of patients for targeted therapies. For example, in patients treated with gefitinib, a low baseline SUV of ¹⁸F-FDG has been associated with a higher response rate (53% vs 18%) and a prolonged PFS – median, 33.1 vs

8.6 weeks (Na *et al*, 2008). In renal cell carcinoma patients treated with sorafenib, a high baseline K^{trans} has been shown to have predictive value and prognostic value with elevated baseline K^{trans} being associated with response and longer PFS (Flaherty *et al*, 2008; Hahn *et al*, 2008). Identifying HER-2 overexpressing breast cancers for treatment with trastuzumab (Tolmachev, 2008) or imaging the oestrogen receptor status (Dehdashti *et al*, 2009) before treatment with aromatase inhibitors are other examples of using molecular imaging as a means of stratifying patients based on target recognition into likely responders and non-responders. Recent studies have demonstrated that in patients with ER+ breast cancer, a higher ¹⁸F-FES (16 α -¹⁸F-fluoroestradiol-17 β) uptake at baseline is predictive of responsiveness to endocrine therapy (Dehdashti *et al*, 2009).

Use of a combination of tumour functional features also may prove to be helpful in patient stratification. For example, the presence of flow-metabolism mismatch has been measured using with a combination of H₂¹⁵O-PET and ¹⁸F-FDG-PET. A low BF (and thus probably low tissue oxygenation) with a high tumour metabolism has been linked with aggressive cancer phenotypes in breast (Dunnwald *et al*, 2008) and pancreatic cancer (Komar *et al*, 2009); in the latter study SUV_{max}/BF ratio was significantly higher in those living <12 months compared with those with survival >12 months, although neither parameter independently was significant between groups.

Identification of tumour hypoxia could facilitate the use of bioreductive drugs, which are metabolised to cytotoxic compounds only in hypoxic cells. Tirapazamine (TPZ) is the most advanced such drug in development and the relatively limited benefit in tumour control in >1100 patients was likely partially due to poor patient stratification with inclusion of patients with better-oxygenated tumours in the trials. A recent report comparing cisplatin/5-FU vs cisplatin/TPZ in which ¹⁸F-FMISO-PET was used to stratify the tumours into hypoxic and non-hypoxic subgroups showed that TPZ improved local control in hypoxic but not in non-hypoxic head and neck tumours (Rischin *et al*, 2006).

IMAGING TO DEFINE DOSE AND/OR SCHEDULE

In the clinic, phase I trials usually incorporate a dose-escalation phase in which imaging does not formally have a role, under the assumption that the biggest imaging changes are likely to be detected at the highest dose, and the objective of this phase is to establish the MTD. However, with targeted agents functional imaging changes are likely to be apparent at lower doses than the MTD because of biological activity of the agent by direct target inhibition. A plateau level at which increasing dose is not followed by an imaging parameter change suggests that imaging may be helpful in choosing the optimal biological dose. Despite this, there are few cases in which imaging parameter changes have helped define the effective dose to take into phase II studies. Examples are K^{trans} change following treatment with sorafenib (Hahn *et al*, 2008) and brivanib (Jonker, 2011), H₂¹⁵O-PET and C¹⁵O-PET information with CA4P treatment. In studies of CA4P, increasing effects on perfusion were noted to plateau at doses ≥ 52 mg m⁻² resulting in a recommended phase II dose of 52–66 mg m⁻², below the MTD dose of 88 mg m⁻² (Anderson *et al*, 2003).

Use of imaging to determine the optimal schedule of a targeted agent or for monitoring drug activity according to the class of therapeutic agent has received very little attention and data are limited. Jonker *et al* (2011) in a study of brivanib, a dual VEGFR and FGFR tyrosine kinase inhibitor, investigators evaluated DCE-MRI responses in several dose schedules in selected patients known to respond to anti-VEGF therapies and then selected the optimal schedule for a phase II trial. A similar approach has been utilised with sorafenib in renal cancer by Hahn *et al* (2008).

Table 1 Summary of the main functional imaging techniques used in phase I clinical trials in which a significant change in imaging parameters following treatment has been observed

Technique	Coverage	Imaging principle	Biological feature explored	Imaging parameters (most used)	Reproducibility	Agent	Target	Time points at which a statistically significant change in imaging parameters has been observed
DCE (dynamic contrast enhanced)-MRI	Single organ; 12–14 slices (6–7 cm)	Changes in T1 signal intensity after administration of low molecular weight contrast agent	Tissue perfusion and vascularity	IAUGC (integrated area under Gadolinium curve) K^{trans} (transfer constant)	wCV = 12–16% $r = 26–30\%$ (Morgan et al, 2006) wCV = 19–29% $r = 30–36\%$ (Morgan et al, 2006) wCV = 24% (Galbraith et al, 2002a) wCV = 9% (Galbraith et al, 2002a)	Axitinib (AG013736) Cediranib (AZD2171) Sorafenib (BAY 43–9006) Intedantib (BIBF-1120) Bivanib (BMS-582664) HuMv833 Vatalanib (PTK787/ZK-222584) Sunitinib (SU11248) CA4P Vadimezan (DMXAA) ZD6126 Bevacizumab Sorafenib (BAY 43-9006) Sunitinib (SU11248)	VEGFR1, 2; PDGFR- β VEGFR1,2,3; PDGFR- α , - β c-KIT Raf-1; wtBRAF; VEGFR2,3; PDGFR- β ; FLT-3; KIT; FGFR-1 VEGFR 1,2,3; FGFR 1, 2,3; PDGFR, Src, Lck, Lyn, FLT-3 VEGFR2, VEGFR3, FGFR1, FGFR2 VEGF VEGFR 2 VEGFR-1, -2; PDGFR β ; KIT; FLT-4; c-FMS Tubulin polymerization; Established tumour blood vessels Colchicin analogue (tubulin binding) Humanized anti-VEGF monoclonal antibody Raf-1; wtBRAF; VEGFR2, -3; PDGFR- β ; FLT-3; KIT; FGFR-1 VEGFR1,2,3; PDGFR- α , - β ; KIT; FLT-3; CSFR-1; RET	2 and 28 days (Liu et al, 2005) 1 and 2 and 5 and 28 and 112 days (Batchelor et al, 2007; Drevs et al, 2007) 12 weeks (Flaherty et al, 2008) 2.7–10.9 weeks (median 6.1) (Hahn et al, 2008) 3 and 30 days (Mross et al, 2010) 2 and 8 and 26 days (Jonker et al, 2011) 48 h and 35 days (Jayson et al, 2002) 2 and 28 and 30 days (Morgan et al, 2003) 14 days (Zhu et al, 2009) 4–6 h and 24 h (Dowlati et al, 2002) 24 h (Galbraith et al, 2002b) 24 h (Evelhoch et al, 2004) 10–12 days (Jiang et al, 2012) 6 weeks (Fournier et al, 2010) 6 weeks (Fournier et al, 2010)
DCE-CT	Single organ 4–8 slices (2.5–5 mm)	Changes in CT density (H-U) following administration of iodinated contrast agent	Tissue perfusion and vascularity	rBV (relative blood volume)	wCV 14–15% $r = 38\%$ (Goh et al, 2006)	Sorafenib (BAY 43-9006) Sunitinib (SU11248)	VEGFR-1, -2; PDGFR β ; KIT; FLT-4; c-FMS	2 and 8 and 26 days (Jonker et al, 2011)
DCE-US	Single lesion single slice	Enhanced representation of the vasculature following administration of microbubbles	Tissue perfusion and vascularity	rBF (relative blood flow) MTT (mean transit time) AUC (area under curve)	wCV = 23% $r = 65\%$ (Goh et al, 2006) $r = 97\%$ (Goh et al, 2006) No data available in clinical studies	Bevacizumab Sorafenib (BAY 43-9006) Sunitinib (SU11248)	Humanized anti-VEGF monoclonal antibody Raf-1; wtBRAF; VEGFR2, -3; PDGFR- β ; FLT-3; KIT; FGFR-1 VEGFR-1, -2, -3; PDGFR- α , β ; KIT; FLT-3; CSFR-1; RET	3 and 7 and 14 and 60 days (Lassau et al, 2011) 3 and 6 weeks (Lamuraglia et al, 2006) 15 days (Lassau et al, 2010)
Diffusion Weighted Magnetic Resonance Imaging (DW-MRI)	Whole organ coverage routinely; whole body diffusion available	Measures water tissue diffusibility by applying two, balanced, opposing magnitude, gradient pulses to a conventional T2w, spin-echo MRI sequence	Indirect assessment of tissue cellularity and presence of necrosis	TPI (time to PI) ADC (apparent diffusion coefficient)	$\rho = 13.3$ (Koh et al, 2009) two centre trial	CA4P Cediranib (AZD 2171)	Tubulin polymerization VEGFR1,2,3; PDGFR- α , - β c-KIT	3 h after 2nd dose (Koh et al, 2009) 1 and 28 and 56 days (Batchelor et al, 2007)
¹⁸ F-FDG (glucose analogue) PET	Whole body	¹⁸ F-FDG enters the cell via glucose transporters, phosphorylated by hexokinase and then trapped within cells	Glucose utilization in tumour cells.	SUV max (standardized unit value)	wCV = 10.7–15.9% $r = -0.34–0.27\%$ to +0.37–52.1% multicenter data $r = 6–10–42\%$	Sorafenib (BAY 43-9006) Sunitinib (SU11248)	Raf-1; wtBRAF; VEGFR2, -3; PDGFR- β ; FLT-3; KIT; FGFR-1 VEGFR-1, -2, -3; PDGFR- α , - β ; KIT; FLT-3; CSFR-1; RET	3 weeks (Siemiernik et al, 2008) 10–14 day (Van den Abbeele et al, 2008) 28 and 56 days (Herbst et al, 2002)
¹⁸ F-FLT (flurothymidine) PET	Whole body	Enter cells via nucleoside transporter; proteins, phosphorylated by thymidine kinase, trapped intracellularly, but not incorporated into DNA	Tissue proliferation rate	SUV mean SUV 41% SUV max	Single centre data acquisition (Naimias and Wahl, 2008; Velásquez et al, 2009) 1–7% (Naimias and Wahl, 2008) ICC = 0.98 (95% CI 0.95–0.99) $r = 15\%$ ICC = 0.93 (95% CI 0.85–0.97) $r = 20–25\%$ (de Langen et al, 2009)	rh-Endo recombinant human endostatin Gefitinib Sunitinib	VEGFR-1, -2, -3; PDGFR- α , - β ; KIT; FLT-3; CSFR-1; RET	2 days and 4 weeks (Sunaga et al, 2008) 4 weeks (Liu et al, 2011)

Table 1 (Continued)

Technique	Coverage	Imaging principle	Biological feature explored	Imaging parameters (most used)	Reproducibility	Agent	Target	Time points at which a statistically significant change in imaging parameters has been observed
$H_2^{15}O$, (labeled H_2O) PET	Whole body	Inhaled $C^{15}O_2$ or intravenous $H_2^{15}O$, reach an equilibrium in which the diffusion rate into the tissue from the arterial blood is balanced by the diffusion rate out of the tissue into venous blood and the rate of radioactive decay of the ^{15}O .	Tissue blood flow and oxygen utilization	Tumour perfusion Regional flow Volume of distribution (VT or V_d)	$r = 15.8-40\%$ (depending on VOI selection method) (van der Veldt et al, 2010) wCV 11% (van der Veldt et al, 2010) $r = 32\%$ (van der Veldt et al, 2010) $r = 36-47\%$ (de Langen et al, 2008)	rh-Endo recombinant human endostatin CA4P	Proliferation and migration of capillary endothelial cells Tubulin polymerization	28 and 56 days (Herbst et al, 2002) 24 h (Anderson et al, 2003)

Abbreviations: ADC = apparent diffusion coefficient; AUC = area under curve; BF = blood flow; CI = confidence interval; CT = computerised tomography; CV = coefficient of variance; DCE = dynamic contrast enhanced; DW = diffusion weighted; 18F-FDG = 18F-fluorodeoxyglucose; 18F-FLT = 18F-fluorothymidine; HU = Hounsfield unit; ICC = interclass correlations; IAUGC = integrated area under gadolinium curve; KIT = mast/stem cell growth factor receptor; MRI = magnetic resonance imaging; MTT = mean transit time; PET = positron emission tomography; PDGFR = platelet derived growth factor receptor; PI = peak intensity; r = reproducibility coefficient; RAFI, BRAF = members of the raf kinases family (raf - rapidly accelerated fibrosarcoma); rBF = relative blood flow; rBV = relative blood volume; SUV = standardised unit value; TPI = time to PI; VEGFR = vascular endothelial growth factor receptor; US = ultrasound; VOI = volume of interest; wtBRAF = wild type BRAF.

OPTIMISING AND STANDARDISING FUNCTIONAL IMAGING READOUTS

Technique reproducibility

Better acquisition techniques for DCE-MRI, quality assurance and improved data modelling have meant that reproducibility figures have improved from over 30% to 26% for IAUGC and from >40% to around 30% for K^{trans} (Table 1).

Preliminary data for DW-MRI suggest that ADC measurements have a reproducibility of ~15% in a multicentre setting (Koh et al, 2009) but it is most likely to range between 8 and 15%, depending on lesion location, acquisition plane and acquisition protocol.

For 1H -MRS reproducibility, data come mainly from brain studies: median coefficient of variance (CV) was 6.2% and 9.7% for serial measurements of NAA and choline, respectively (Maudsley et al, 2010). In the liver measurements of choline are challenged by large contaminant lipid peaks and patient motion.

Reported thresholds for ^{18}F -FDG-PET for determining metabolic changes being approximately -34% to +52% for individual centres and -27% to +37% after centralised QA (Velasquez et al, 2009). For $H_2^{15}O$ -PET, two small oncological studies, have reported wCV of 10-11% for breast and abdominal tumours (de Langen et al, 2008).

Other described techniques lack reproducibility data.

Data analysis technique

Traditionally, a single target lesion was chosen for analysis based on its location, size and morphology (ideally >2.5 cm but <5 cm with <50% necrosis, in a location not greatly influenced by movement or artefacts). To account for differential response in phase I trials (Figure 3), identification of several lesions with different characteristics is preferred to include a spectrum of potential drug effects. This can be achieved with whole body scanning: whole-body PET is widely used and sliding table techniques with faster sequences in MRI have also enabled whole-body MRI in <60 min. Separate analysis of tumours subregions may also detect differential drug effects such as rim vs core differential effects in antiangiogenic therapy, which maybe missed on whole tumour analysis.

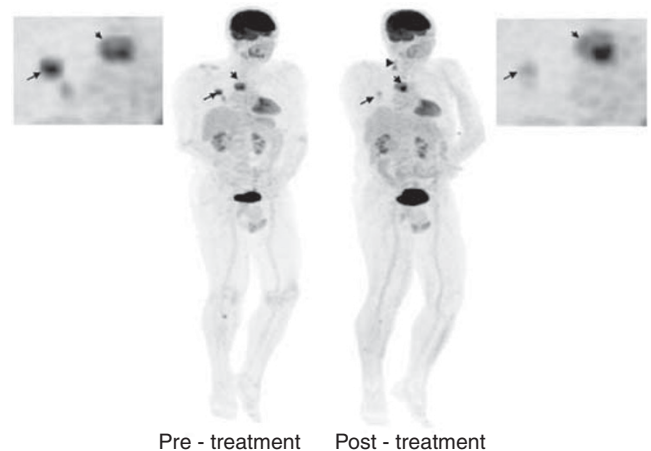


Figure 3 Differential response in ^{18}F -FDG PET uptake after 1 cycle of targeted therapy with a bRaf and Mek inhibitor in a patient with metastatic melanoma. The mediastinal nodal mass has increased in size and demonstrates a heterogeneous increase in SUV (short arrow) while lung nodules are smaller in size and show significant reduction in SUV (long arrow). The tibial bony lesion seen on the pre-treatment scan is smaller, but a new tibial lesion is visible. The new cervical nodes (arrowhead) were felt to be inflammatory in aetiology.

Summary parameters such as mean and median values oversimplify data and may mask critical information concerning tumour heterogeneity. Histogram, fractal and principal component analysis are viable alternatives. Parametric response maps (PRMs) are novel methods of image analysis using a voxel-by-voxel approach that can be applied to various functional imaging techniques such as perfusion or ADC maps. Two imaging volume data sets (e.g., baseline and early response) are co-registered and computationally analysed to yield PRM, which are generally colour coded based on the magnitude and direction of the parameter change. The changes can be displayed as histograms or scatter plots. In malignant brain tumours, PRM_{ADC} obtained 3 weeks and PRM_{rFBV} and PRM_{rBF} at 1 and 3 weeks into conventional therapy was prognostic for later radiographic response, time to progression and overall survival (OS) whereas percentage change in mean parameters (ADC, relative BV and relative BF) was less significant (Galbán *et al*, 2009a). Similar findings have also been reported using PRM_{ADC} in head and neck tumours (Galbán *et al*, 2009b) and assessment of metastatic bony disease in prostate cancer (Reischauer *et al*, 2010). These methods of data analysis are still in early stages of development and evaluation.

Multiparametric imaging

Targeted molecular approaches typically seek to inhibit specific pathways or molecules deemed to have an important role in tumour progression. Most of the preclinical data comes from relatively 'homogenous' cell lines and xenografts. In contrast, patients enrolled in phase I trials are heavily pre-treated and have heterogenous tumours that may behave differently from the original primary and vary between sites of disease. A multiparametric approach using a combination of imaging biomarkers is more informative than a single imaging biomarker; for example, a composite 'vascular normalisation index' integrating K^{trans} , CBV and plasma collagen IV after one dosing of

cediranib has been shown to correlate with PFS and OS in patients with recurrent glioblastoma (Sorensen *et al*, 2009). Multiparametric MRI data (DCE-MRI, DW-MRI, MRS and ISW-MRI) through a target volume can be acquired in 50–60 min (Figure 4).

Defining criteria of response using functional imaging indices

Imaging criteria of response to date have relied on size evaluation as this has been shown to equate to improved clinical outcome. With functional imaging, new definitions of response need to be set and equated with PFS and OS. In the first instance, levels of change >95% confidence intervals of baseline variability (from reproducibility studies) for each technique need to be set in order to measure treatment-induced changes that specifically relate to drug activity. Although available studies are small and confounded by inter-patient heterogeneity, generally data show that patients whose tumours undergo at least a 50% reduction in DCE-MRI parameters attain stable disease or response by RECIST; also, DCE-MRI can differentiate tumour progression from treatment-induced changes in the brain with 95% sensitivity and 78% specificity (Narang *et al*, 2011).

Data on the expected magnitude of change in ADC indicative of response to standard therapy are becoming available for rectal, liver, lung and ovary tumours. It is likely that an increase in 20–25% after 1 week of treatment and at least 40% at later time points (3–4 weeks) of treatment will be indicative into tumour response (Sun *et al*, 2011). In bone, as with soft tissue tumours an increase in ADC occurs in responding lesions but because of the contribution of low ADC values from marrow fat in response, this requires more complex analysis (Messiou *et al*, 2011).

As with MRI, response assessment in ¹⁸F-FDG-PET requires a consistent methodology to allow quantitative assessments. EORTC guidelines published in 1999 suggested that medically relevant beneficial changes are often associated with a 30% or greater

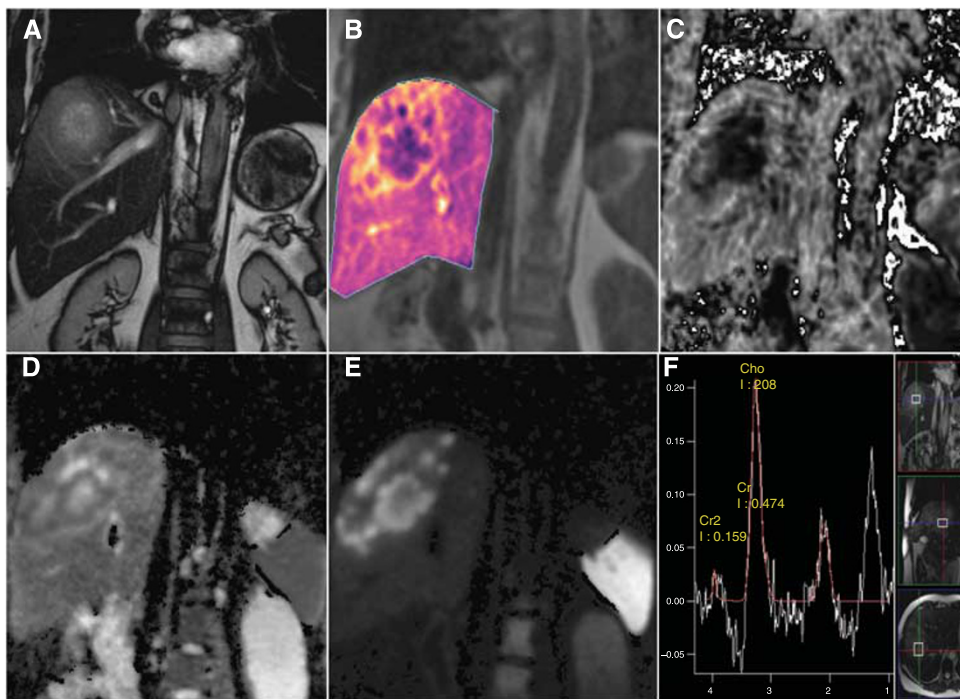


Figure 4 Multiparametric MRI protocol in the coronal plane in a patient with liver metastases from colon cancer showing a combination of anatomical information (T2-weighted, **A**) with functional imaging parametric maps, which quantify tumour vascularity (K^{trans} , **B**), areas of hypoxia ($R2^*$ maps, **C**) and tumour cellularity (ADC and DWI, **D** and **E**, respectively) together with single voxel ¹H-MRS (**F**). The metastasis shows a vascular (**B**), hypercellular (**D** and **E**) rim with a hypoxic (**C**), necrotic (**D**) centre with increased proliferative activity as evidenced by choline signal in (**F**).

decline. PERCIST criteria that recommend SUV evaluation in the most active region of metabolically active tumours and include RECIST 1.1 in cases that do not have ^{18}F -FDG avidity have been also been proposed (Wahl *et al*, 2009).

SUMMARY AND CONCLUSION

There is a clear need for robust functional imaging readouts to effectively assess novel cancer therapeutics and stratify patients to appropriate therapies. The tools to characterise a tumour phenotype on imaging based on vascularity, cellularity, metabolism and hypoxia exist but more specific targeted molecular profiling is still in its infancy. Development of dedicated tracers to identify receptor status will allow mapping of the whole tumour burden and its heterogeneity.

In the context of phase I trials, functional imaging should be performed at least in the expansion phase in order that it can inform and assist in the evaluation of target inhibition, patient selection and anti-tumour activity. Imaging methods should be relevant to the targeted pathway and specialist radiologist input is essential at the stage of trial design and set-up to ensure that the imaging protocol is designed accordingly.

We therefore recommend that perfusion imaging should be routinely incorporated into trials of agents targeting tumour vasculature as a biomarker of antiangiogenic activity and techniques such as ^{18}F -FDG-PET should also be considered for early clinical trials of inhibitors of specific pathways, such as

PI3K/AKT/MTOR. DW-MRI provides a biomarker for apoptosis and cell death and before enrolling a patient in a trial with a bio-reductive agent, the hypoxic status of the tumour should be imaged with ^{18}F -Miso. The evidence for other tracers such as ^{18}F -FLT-PET does not warrant routine use. As receptor imaging techniques, (e.g., Her2 receptor status), mature they will prove invaluable for patient selection and treatment monitoring.

Currently, the use of functional imaging in large-scale multi-centre clinical trials is prohibited by the limited technique reproducibility between centres and scanners, inadequate standardisation of data acquisition and analysis techniques and lack of necessary skills outside large centres. These obstacles are being addressed by programs such as the EU innovative medicine initiative in imaging, which should achieve standardisation of acquisition and analysis methodology for functional imaging biomarkers. There is an urgent need to strengthen the evidence base and increase familiarity with functional imaging techniques, through both single and multicentre studies.

ACKNOWLEDGEMENTS

We acknowledge the support received from Cancer Research UK, EPSRC Cancer Imaging Centre and Experimental Cancer Medicine Centre in association with the MRC and Department of Health (England) Grant C1060/A10334, and NHS funding to the National Institute for Health Research Biomedical Research Centre.

REFERENCES

- Anderson HL, Yap JT, Miller MP, Robbins A, Jones T, Price PM (2003) Assessment of pharmacodynamic vascular response in a phase I trial of combretastatin A4 phosphate. *J Clin Oncol* 21(15): 2823–2830
- Baek HM, Chen JH, Nie K, Yu HJ, Bahri S, Mehta RS, Nalcioglu O, Su MY (2009) Predicting pathologic response to neoadjuvant chemotherapy in breast cancer by using MR imaging and quantitative ^1H MR spectroscopy. *Radiology* 251(3): 653–662
- Barwick T, Bencherif B, Mountz JM, Avril N (2009) Molecular PET and PET/CT imaging of tumour cell proliferation using F-18 fluoro-L-thymidine: a comprehensive evaluation. *Nucl Med Commun* 30(12): 908–917
- Batchelor TT, Sorensen AG, di Tomaso E, Zhang WT, Duda DG, Cohen KS, Kozak KR, Cahill DP, Chen PJ, Zhu M, Ancukiewicz M, Mrugala MM, Plotkin S, Drappatz J, Louis DN, Ivy P, Scadden DT, Benner T, Loeffler JS, Wen PY, Jain RK (2007) AZD2171, a pan-VEGF receptor tyrosine kinase inhibitor, normalizes tumor vasculature and alleviates edema in glioblastoma patients. *Cancer Cell* 11(1): 83–95
- Belouche-Babari M, Chung YL, Al-Saffar NM, Falck-Miniotis M, Leach MO (2010) Metabolic assessment of the action of targeted cancer therapeutics using magnetic resonance spectroscopy. *Br J Cancer* 102(1): 1–7
- Broillet A, Hantson J, Ruegg C, Messager T, Schneider M (2005) Assessment of microvascular perfusion changes in a rat breast tumor model using SonoVue to monitor the effects of different anti-angiogenic therapies. *Acad Radiol* 12(Suppl 1): S28–S33
- Cai W, Sam Gambhir S, Chen X (2005) Multimodality tumor imaging targeting integrin $\alpha\text{v}\beta_3$. *Biotechniques* 39(6 Suppl): S14–S25
- de Langen AJ, Klabbars B, Lubberink M, Boellaard R, Spreuwenberg MD, Slotman BJ, de Bree R, Smit EF, Hoekstra OS, Lammertsma AA (2009) Reproducibility of quantitative ^{18}F -3'-deoxy-3'-fluorothymidine measurements using positron emission tomography. *Eur J Nucl Med Mol Imaging* 36(3): 389–395
- de Langen AJ, Lubberink M, Boellaard R, Spreuwenberg MD, Smit EF, Hoekstra OS, Lammertsma AA (2008) Reproducibility of tumor perfusion measurements using ^{15}O -labeled water and PET. *J Nucl Med* 49(11): 1763–1768
- Dehdashti F, Mortimer JE, Trinkaus K, Naughton MJ, Ellis M, Katzenellenbogen JA, Welch MJ, Siegel BA (2009) PET-based estradiol challenge as a predictive biomarker of response to endocrine therapy in women with estrogen-receptor-positive breast cancer. *Breast Cancer Res Treat* 113: 509–517
- Donaldson SB, Betts G, Bonington SC, Homer JJ, Slevin NJ, Kershaw LE, Valentine H, West CM, Buckley DL (2011) Perfusion Estimated With Rapid Dynamic Contrast-Enhanced Magnetic Resonance Imaging Correlates Inversely With Vascular Endothelial Growth Factor Expression and Pimonidazole Staining in Head-and-Neck Cancer: A Pilot Study. *Int J Radiat Oncol Biol Phys* 81(4): 1176–1183
- Dowlati A, Robertson K, Cooney M, Petros WP, Stratford M, Jesberger J, Rafie N, Overmoyer B, Makkar V, Stambler B, Taylor A, Waas J, Lewin JS, McCrae KR, Remick SC (2002) A phase I pharmacokinetic and translational study of the novel vascular targeting agent combretastatin a-4 phosphate on a single-dose intravenous schedule in patients with advanced cancer. *Cancer Res* 62(12): 3408–3416
- Dreves J, Siegert P, Medinger M, Mross K, Strecker R, Zirrgiebel U, Harder J, Blum H, Robertson J, Jurgensmeier JM, Puchalski TA, Young H, Saunders O, Unger C (2007) Phase I clinical study of AZD2171, an oral vascular endothelial growth factor signaling inhibitor, in patients with advanced solid tumors. *J Clin Oncol* 25(21): 3045–3054
- Dunnwald LK, Gralow JR, Ellis GK, Livingston RB, Linden HM, Specht JM, Doot RK, Lawton TJ, Barlow WE, Kurland BF, Schubert EK, Mankoff DA (2008) Tumor metabolism and blood flow changes by positron emission tomography: relation to survival in patients treated with neoadjuvant chemotherapy for locally advanced breast cancer. *Journal of Clinical Oncology* 26: 4449–4457
- Erber R, Thurnher A, Katsen AD, Groth G, Kerger H, Hammes H-P, Menger MD, Ullrich A, Vajkoczy P (2004) Combined inhibition of VEGF and PDGF signaling enforces tumor vessel regression by interfering with pericyte-mediated endothelial cell survival mechanisms. *FASEB J* 18: 338–340
- Evelhoch JL, LoRusso PM, He Z, DelProposto Z, Polin L, Corbett TH, Langmuir P, Wheeler C, Stone A, Leadbetter J, Ryan AJ, Blakey DC, Waterton JC (2004) Magnetic resonance imaging measurements of the response of murine and human tumors to the vascular-targeting agent ZD6126. *Clin Cancer Res* 10(11): 3650–3657
- Flaherty KT, Rosen MA, Heitjan DF, Gallagher ML, Schwartz B, Schnall MD, O'Dwyer PJ (2008) Pilot study of DCE-MRI to predict progression-free survival with sorafenib therapy in renal cell carcinoma. *Cancer Biol Ther* 7(4): 496–501

- Fournier LS, Oudard S, Thiam R, Trinquart L, Banu E, Medioni J, Balvay D, Chatellier G, Frija G, Cuenod CA (2010) Metastatic renal carcinoma: evaluation of antiangiogenic therapy with dynamic contrast-enhanced CT. *Radiology* 256(2): 511–518
- Galbán C, Chenevert T, Meyer C, Tsien C, Lawrence T, Hamstra D, Junck L, Sundgren P, Johnson T, Ross D, Rehemtulla A, Ross B (2009a) The parametric response map is an imaging biomarker for early cancer treatment outcome. *Nat Med* 15: 572–576
- Galbán C, Mukherji S, Chenevert T, Meyer C, Hamstra D, Bland P, Johnson T, Moffat B, Rehemtulla A, Eisbruch A, Ross B (2009b) A feasibility study of parametric response map analysis of diffusion-weighted magnetic resonance imaging scans of head and neck cancer patients for providing early detection of therapeutic efficacy. *Translational oncology* 2: 184–190
- Galbraith S, Maxwell R, Lodge M, Tozer G, Wilson J, Taylor N, Stirling J, Sena L, Padhani A, Rustin G (2003) Combretastatin A4 phosphate has tumor antivascular activity in rat and man as demonstrated by dynamic magnetic resonance imaging. *J Clin Oncol* 21: 2831–2842
- Galbraith SM, Lodge MA, Taylor NJ, Rustin G, Bentzen S, Stirling JJ, Padhani AR (2002a) Reproducibility of dynamic contrast-enhanced MRI in human muscle and tumours: comparison of quantitative and semi-quantitative analysis. *NMR Biomed* 15(2): 132–142
- Galbraith SM, Rustin G, Lodge MA, Taylor NJ, Stirling JJ, Jameson M, Thompson P, Hough D, Gumbrell L, Padhani AR (2002b) Effects of 5,6-dimethylxanthenone-4-acetic acid on human tumor microcirculation assessed by dynamic contrast-enhanced magnetic resonance imaging. *J Clin Oncol* 20(18): 3826–3840
- Goh V, Halligan S, Hugill JA, Bartram CI (2006) Quantitative assessment of tissue perfusion using MDCT: comparison of colorectal cancer and skeletal muscle measurement reproducibility. *AJR Am J Roentgenol* 187(1): 164–169
- Hahn OM, Yang C, Medved M, Karczmar G, Kistner E, Karrison T, Manchen E, Mitchell M, Ratain MJ, Stadler WM (2008) Dynamic contrast-enhanced magnetic resonance imaging pharmacodynamic biomarker study of sorafenib in metastatic renal carcinoma. *J Clin Oncol* 26(28): 4572–4578
- Herbst RS, Mullani NA, Davis DW, Hess KR, McConkey DJ, Charnsangavej C, O'Reilly MS, Kim H-W, Baker C, Roach J, Ellis LM, Rashid A, Pluda J, Bucana C, Madden TL, Tran HT, Abbruzzese JL (2002) Development of biologic markers of response and assessment of antiangiogenic activity in a clinical trial of human recombinant endostatin. *J Clin Oncol* 20: 3804–3814
- Jayson GC, Zweit J, Jackson A, Mulatero C, Julyan P, Ranson M, Broughton L, Wagstaff J, Hakansson L, Groenewegen G, Bailey J, Smith N, Hastings D, Lawrence J, Haroon H, Ward T, McGown AT, Tang M, Levitt D, Marreaud S, Lehmann FF, Herold M, Zwierzina H, Group EO/RaToCBTD (2002) Molecular imaging and biological evaluation of HuMV833 anti-VEGF antibody: implications for trial design of antiangiogenic antibodies. *J Natl Cancer Inst* 94: 1484–1493
- Jiang T, Kambadakone A, Kulkarni NM, Zhu AX, Sahani DV (2012) Monitoring response to antiangiogenic treatment and predicting outcomes in advanced hepatocellular carcinoma using image biomarkers, CT perfusion, tumor density, and tumor size (RECIST). *Invest Radiol* 47(1): 11–17
- Jonker DJ, Rosen LS, Sawyer MB, de Braud F, Wilding G, Sweeney CJ, Jayson GC, McArthur GA, Rustin G, Goss G, Kantor J, Velasquez L, Syed S, Mokliatchouk O, Feltruate DM, Kollia G, Nuyten DS, Galbraith S (2011) A phase I study to determine the safety, pharmacokinetics and pharmacodynamics of a dual VEGFR and FGFR inhibitor, brivanib, in patients with advanced or metastatic solid tumors. *Ann Oncol* 22(6): 1413–1419
- Jordan B, Runquist M, Raghunand N, Baker A, Williams R, Kirkpatrick L, Powis G, Gillies R (2005) Dynamic contrast-enhanced and diffusion MRI show rapid and dramatic changes in tumor microenvironment in response to inhibition of HIF-1 α using PX-478. *Neo* 7: 475–485
- Koh DM, Blackledge M, Collins DJ, Padhani AR, Wallace T, Wilton B, Taylor NJ, Stirling JJ, Sinha R, Walicke P, Leach MO, Judson I, Nathan P (2009) Reproducibility and changes in the apparent diffusion coefficients of solid tumours treated with combretastatin A4 phosphate and bevacizumab in a two-centre phase I clinical trial. *Eur Radiol* 19(11): 2728–2738
- Kola I, Landis J (2004) Can the pharmaceutical industry reduce attrition rates? *Nat Rev Drug Discov* 3: 711–715
- Komar G, Kauhanen S, Liukka K, Seppanen M, Kajander S, Ovaska J, Nuutila P, Minn H (2009) Decreased Blood Flow with Increased Metabolic Activity: A Novel Sign of Pancreatic Tumor Aggressiveness. *Clinical Cancer Research* 15: 5511–5517
- Lamuraglia M, Bridal SL, Santin M, Izzi G, Rixe O, Paradiso A, Lucidarme O (2010) Clinical relevance of contrast-enhanced ultrasound in monitoring anti-angiogenic therapy of cancer: current status and perspectives. *Crit Rev Oncol Hematol* 73(3): 202–212
- Lamuraglia M, Escudier B, Chami L, Schwartz B, Leclere J, Roche A, Lassau N (2006) To predict progression-free survival and overall survival in metastatic renal cancer treated with sorafenib: pilot study using dynamic contrast-enhanced Doppler ultrasound. *Eur J Cancer* 42(15): 2472–2479
- Lane H, Wood J, McSheehy P, Allegrini P, Boulay A, Brueggen J, Littlewood-Evans A, Maira S-M, Martiny-Baron G, Schnell C, Sini P, O'Reilly T (2009) mTOR inhibitor RAD001 (everolimus) has antiangiogenic/vascular properties distinct from a VEGFR tyrosine kinase inhibitor. *Clin Cancer Res* 15: 1612–1622
- Lassau N, Koscielny S, Albiges L, Chami L, Benatsou B, Chebil M, Roche A, Escudier BJ (2010) Metastatic renal cell carcinoma treated with sunitinib: early evaluation of treatment response using dynamic contrast-enhanced ultrasonography. *Clin Cancer Res* 16: 1216–1225
- Lassau N, Koscielny S, Chami L, Chebil M, Benatsou B, Roche A, Ducreux M, Malka D, Boige V (2011) Advanced hepatocellular carcinoma: early evaluation of response to bevacizumab therapy at dynamic contrast-enhanced US with quantification—preliminary results. *Radiology* 258(1): 291–300
- Lavisse S, Lejeune P, Rouffiac V, Elie N, Bribes E, Demers B, Vrignaud P, Bissery M-C, Brulé A, Koscielny S, Péronneau P, Lassau N (2008) Early quantitative evaluation of a tumor vasculature disruptive agent AVE8062 using dynamic contrast-enhanced ultrasonography. *Investigative radiology* 43: 100–111
- Leach MO, Brindle KM, Evelhoch JL, Griffiths JR, Horsman MR, Jackson A, Jayson GC, Judson IR, Knopp MV, Maxwell RJ, McIntyre D, Padhani AR, Price P, Rathbone R, Rustin GJ, Tofts PS, Tozer GM, Vennart W, Waterton JC, Williams SR, Workman P (2005) The assessment of antiangiogenic and antivascular therapies in early-stage clinical trials using magnetic resonance imaging: issues and recommendations. *Br J Cancer* 92(9): 1599–1610
- Liu G, Jeraj R, Vanderhoek M, Perlman S, Kolesar J, Harrison M, Simoncic U, Eickhoff J, Carmichael L, Chao B, Marnocha R, Ivy P, Wilding G (2011) Pharmacodynamic study using FLT PET/CT in patients with renal cell cancer and other solid malignancies treated with sunitinib malate. *Clin Cancer Res* 17(24): 7634–7644
- Liu G, Rugo HS, Wilding G, McShane TM, Evelhoch JL, Ng C, Jackson E, Kelcz F, Yeh BM, Lee Jr FT, Charnsangavej C, Park JW, Ashton EA, Steinfeldt HM, Pithavala YK, Reich SD, Herbst RS (2005) Dynamic contrast-enhanced magnetic resonance imaging as a pharmacodynamic measure of response after acute dosing of AG-013736, an oral angiogenesis inhibitor, in patients with advanced solid tumors: results from a phase I study. *J Clin Oncol* 23(24): 5464–5473
- Ma WW, Jacene H, Song D, Vildardell F, Messersmith WA, Laheru D, Wahl R, Endres C, Jimeno A, Pomper MG, Hidalgo M (2009) [18F]fluorodeoxyglucose positron emission tomography correlates with Akt pathway activity but is not predictive of clinical outcome during mTOR inhibitor therapy. *J Clin Oncol* 27(16): 2697–2704
- Maudsley AA, Domenig C, Sheriff S (2010) Reproducibility of serial whole-brain MR spectroscopic imaging. *NMR Biomed* 23: 251–256
- Mees G, Dierckx R, Vangestel C, Van de Wiele C (2009) Molecular imaging of hypoxia with radiolabelled agents. *Eur J Nucl Med Mol Imaging* 36(10): 1674–1686
- Messiou C, Collins DJ, Giles S, de Bono JS, Bianchini D, de Souza NM (2011) Assessing response in bone metastases in prostate cancer with diffusion weighted MRI. *Eur Radiol* 21: 2169–2177
- Morgan B, Thomas AL, Drevs J, Hennig J, Buchert M, Jivan A, Horsfield MA, Mross K, Ball HA, Lee L, Mielowski W, Fuxuis S, Unger C, O'Byrne K, Henry A, Cherryman GR, Laurent D, Dugan M, Marme D, Steward WP (2003) Dynamic contrast-enhanced magnetic resonance imaging as a biomarker for the pharmacological response of PTK787/ZK 222584, an inhibitor of the vascular endothelial growth factor receptor tyrosine kinases, in patients with advanced colorectal cancer and liver metastases: results from two phase I studies. *J Clin Oncol* 21(21): 3955–3964
- Morgan B, Utting JF, Higginson A, Thomas AL, Steward WP, Horsfield MA (2006) A simple, reproducible method for monitoring the treatment of tumours using dynamic contrast-enhanced MR imaging. *Br J Cancer* 94(10): 1420–1427
- Mross K, Stefanic M, Gmehling D, Frost A, Baas F, Unger C, Strecker R, Henning J, Gaschler-Markefski B, Stopfer P, de Rossi L, Kaiser R (2010)

- Phase I study of the angiogenesis inhibitor BIBF 1120 in patients with advanced solid tumors. *Clin Cancer Res* 16(1): 311–319
- Na II, Byun B, Kang H, Cheon G, Koh J, Kim C, Choe D, Ryoo B, Lee J, Lim S, Yang S (2008) 18F-fluoro-2-deoxy-glucose uptake predicts clinical outcome in patients with gefitinib-treated non-small cell lung cancer. *Clin Cancer Res* 14: 2036–2041
- Nahmias C, Wahl LM (2008) Reproducibility of standardized uptake value measurements determined by 18F-FDG PET in malignant tumors. *J Nucl Med* 49(11): 1804–1808
- Narang J, Jain R, Arbab AS, Mikkelsen T, Scarpace L, Rosenblum ML, Hearshen D, Babajani-Feremi A (2011) Differentiating treatment-induced necrosis from recurrent/progressive brain tumor using non-model-based semiquantitative indices derived from dynamic contrast-enhanced T1-weighted MR perfusion. *Neuro Oncol* 13(9): 1037–1046
- Padhani AR, Krohn KA, Lewis JS, Alber M (2007) Imaging oxygenation of human tumours. *Eur Radiol* 17(4): 861–872
- Padhani AR, Liu G, Koh DM, Chenevert TL, Thoeny HC, Takahara T, Dzik-Jurasz A, Ross BD, Van Cauteren M, Collins D, Hammoud DA, Rustin GJ, Taouli B, Choyke PL (2009) Diffusion-weighted magnetic resonance imaging as a cancer biomarker: consensus and recommendations. *Neoplasia* 11(2): 102–125
- Pope WB, Young JR, Ellingson BM (2011) Advances in MRI assessment of gliomas and response to anti-VEGF therapy. *Curr Neurol Neurosci Rep* 11(3): 336–344
- Reischauer C, Froehlich JM, Koh DM, Graf N, Padevit C, John H, Binkert CA, Boesiger P, Gutzzeit A (2010) Bone metastases from prostate cancer: assessing treatment response by using diffusion-weighted imaging and functional diffusion maps—initial observations. *Radiology* 257(2): 523–531
- Rischin D, Hicks RJ, Fisher R, Binns D, Corry J, Porceddu S, Peters LJ (2006) Prognostic significance of [18F]-misonidazole positron emission tomography-detected tumor hypoxia in patients with advanced head and neck cancer randomly assigned to chemoradiation with or without tirapazamine: a substudy of Trans-Tasman Radiation Oncology Group Study 98.02. *J Clin Oncol* 24(13): 2098–2104
- Schnell C, Stauffer F, Allegrini P, O'Reilly T, McSheehy P, Dartois C, Stumm M, Cozens R, Littlewood-Evans A, Garcia-Echeverria C, Maira S-M (2008) Effects of the dual phosphatidylinositol 3-kinase/mammalian target of rapamycin inhibitor NVP-BEZ235 on the tumor vasculature: implications for clinical imaging. *Cancer Research* 68: 6598–6607
- Shankar LK, Hoffman JM, Bacharach S, Graham MM, Karp J, Lammertsma AA, Larson S, Mankoff DA, Siegel BA, Van den Abbeele A, Yap J, Sullivan D (2006) Consensus recommendations for the use of 18F-FDG PET as an indicator of therapeutic response in patients in National Cancer Institute Trials. *J Nucl Med* 47(6): 1059–1066
- Siemerink E, Mulder NH, Brouwers AH, Hospers GA (2008) Early prediction of response to sorafenib treatment in patients with hepatocellular carcinoma (HCC) with 18F-fluorodeoxyglucose-positron emission tomography (18F-FDG-PET). *Journal of Clinical Oncology* 26: 15600
- Sohn H, Yang Y, Ryu J, Oh S, Im K, Moon D, Lee D, Suh C, Lee J, Kim S (2008) [18F]Fluorothymidine positron emission tomography before and 7 days after gefitinib treatment predicts response in patients with advanced adenocarcinoma of the lung. *Clin Cancer Res* 14: 7423–7429
- Sorensen AG, Batchelor TT, Zhang W-T, Chen P-J, Yeo P, Wang M, Jennings D, Wen PY, Lahdenranta J, Ancukiewicz M, di Tomaso E, Duda DG, Jain RK (2009) A 'vascular normalization index' as potential mechanistic biomarker to predict survival after a single dose of cediranib in recurrent glioblastoma patients. *Cancer Research* 69: 5296–5300
- Souvatoglou M, Grosu AL, Roper B, Krause BJ, Beck R, Reischl G, Picchio M, Machulla HJ, Wester HJ, Piert M (2007) Tumour hypoxia imaging with [18F]FAZA PET in head and neck cancer patients: a pilot study. *Eur J Nucl Med Mol Imaging* 34(10): 1566–1575
- Sun YS, Cui Y, Tang L, Qi LP, Wang N, Zhang XY, Cao K, Zhang XP (2011) Early evaluation of cancer response by a new functional biomarker: apparent diffusion coefficient. *AJR Am J Roentgenol* 197(1): W23–W29
- Sunaga N, Oriuchi N, Kaira K, Yanagitani N, Tomizawa Y, Hisada T, Ishizuka T, Endo K, Mori M (2008) Usefulness of FDG-PET for early prediction of the response to gefitinib in non-small cell lung cancer. *Lung Cancer* 59(2): 203–210
- Tolmachev V (2008) Imaging of HER-2 overexpression in tumors for guiding therapy. *Curr Pharm Des* 14: 2999–3019
- Van den Abbeele AD, Yap JT, Rastarhuyeva I, Akhurst T, Keohan ML, George S, Bhuchar G, Morgan JA, Demetri GD, Maki RG (2008) Early metabolic response to continuous daily dosing of sunitinib in soft tissue sarcomas (STS) other than GIST using FDG-PET. *J Clin Oncol* 26 abstr 10529
- van der Veldt AA, Hendrikse NH, Harms HJ, Comans EF, Postmus PE, Smit EF, Lammertsma AA, Lubberink M (2010) Quantitative parametric perfusion images using 15O-labeled water and a clinical PET/CT scanner: test-retest variability in lung cancer. *J Nucl Med* 51(11): 1684–1690
- Velasquez LM, Boellaard R, Kolia G, Hayes W, Hoekstra OS, Lammertsma AA, Galbraith SM (2009) Repeatability of 18F-FDG PET in a multicenter phase I study of patients with advanced gastrointestinal malignancies. *J Nucl Med* 50: 1646–1654
- Wahl R, Jacene H, Kasamon Y, Lodge M (2009) From RECIST to PERCIST: Evolving Considerations for PET response criteria in solid tumors. *Journal of Nuclear Medicine* 50(Suppl 1): 122S–150S
- Zhu AX, Sahani DV, Duda DG, di Tomaso E, Ancukiewicz M, Catalano OA, Sindhvani V, Blaszkowsky LS, Yoon SS, Lahdenranta J, Bhargava P, Meyerhardt J, Clark JW, Kwak EL, Hezel AF, Miksad R, Abrams TA, Enzinger PC, Fuchs CS, Ryan DP, Jain RK (2009) Efficacy, safety, and potential biomarkers of sunitinib monotherapy in advanced hepatocellular carcinoma: a phase II study. *J Clin Oncol* 27(18): 3027–3035
- Zweifel M, Padhani AR (2010) Perfusion MRI in the early clinical development of antivascular drugs: decorations or decision making tools? *Eur J Nucl Med Mol Imaging* 37(Suppl 1): S164–S182